to that of the parent phenol–carbon monoxide dimer. The spectral shifts for complexes between ortho-substituted phenols and CO are consistent with a bifurcated hydrogen-bonded structure. The limited data correlate with the intrinsic acidity of phenols. This is not unreasonable considering the nonpolar properties of solid argon. A significant portion of the complex is formed upon deposition as a result of surface diffusion. The importance of this work is that it provides information as to how substituent effects and acidity are expressed at cryogenic temperatures in a rare-gas matrix. It would be interesting to determine whether such complexes can be detected in the gas phase.

Acknowledgment. We gratefully acknowledge generous financial support from the National Science Foundation, Grant No. CHE 7811563, and the expert assistance of Dr. Helmut Nickels. We also thank Mrs. Lynda Jacob for her skillful assistance in the preparation of this manuscript.

Registry No. 1, 630-08-0; **2**, 108-95-2; **3**, 371-41-5; **4**, 106-48-9; **5**, 106-41-2; **6**, 150-76-5; **7**, 108-43-0; **8**, 591-20-8; **9**, 372-20-3; **11**, 95-57-8; **12**, 95-56-7; **13**, 90-05-1; **14**, 611-20-1; **17**, 87-65-0; *p*-cresol, 106-44-5.

Kinetics and Mechanism of Molecular A-Frame Formation in Reactions of $[Pt_2(PPh_3)_2(\mu\text{-dppm})_2](PF_6)_2$ with Diazomethane, Carbon Monoxide, Sulfur Dioxide, Sulfur, and Hydrogen Chloride

S. Muralidharan and James H. Espenson*

Contribution from the Ames Laboratory and the Department of Chemistry, Iowa State University, Ames, Iowa 50011. *Received May 14, 1984*

Abstract: The mechanism of the formation of "A" frames of the type $[Pt_2(PPh_3)_2(\mu\text{-Y})(\mu\text{-dppm})_2](PF_6)_2$ (Y = CH_2, CO, S, SO_2) from $[Pt_2(PPh_3)_2(\mu\text{-dppm})_2](PF_6)_2$ by reaction with CH_2N_2, CO, S, and SO_2 (R) in CH_2Cl_2 and other organic solvents has been investigated by using kinetic studies and product analysis. Pseudo-first-order kinetic data (excess $[R]_0$) are consistent with either preequilibrium association of R with the complex prior to rate-limiting product formation or unimolecular formation of a common intermediate which is then attacked by R to form the "A"-frame product. Kinetic studies with $[R]_0 \leq [\text{complex}]_0$ substantiate the latter. The most likely intermediate leading to the products is one with a dangling dppm ligand formed by Pt–P bond heterolysis. When $[R]_0$ is very large, formation of this intermediate becomes rate limiting and is independent of the nature of R, with $k = 2.73 \pm 0.05 \times 10^{-2}\ s^{-1}$ (at 25 °C; $\Delta H^{\ddagger} = 25.0$ kcal mol^{-1} and $\Delta S^{\ddagger} = 18.5$ cal mol^{-1} K^{-1}). The same process and mechanism is observed for R = HCl, although with minor numerical differences; similar salt and solvent polarity effects occur in all of the reactions.

The dimeric platinum(I) and palladium(I) complexes with bridging bis(diphenylphosphino)methane (dppm) ligands, such as $Pt_2Cl_2(\mu\text{-dppm})_2$, are among the rapidly growing number of binuclear compounds which form A-frames.[1-3] Among other reasons, interest in these novel compounds is aroused by their resemblance to intermediates in Fischer–Tropsch reactions and other catalytic processes.[3-6] The process by which small groups are "inserted into" the metal–metal bond of the parent dinuclear complex has been well characterized in a preparative and structural sense.[7-14]

Relatively little is known about the mechanism(s) such reactions follow, however, although the kinetics of insertion of CH_2 upon reaction with diazomethane into the platinum–platinum bond of $Pt_2Cl_2(\mu\text{-dppm})_2$ (eq 1) and such analogues as $[Pt_2Cl(CO)(\mu\text{-dppm})_2]^+$ and $[Pt_2(CO)_2(\mu\text{-dppm})_2]^{2+}$, has recently been examined.[15]

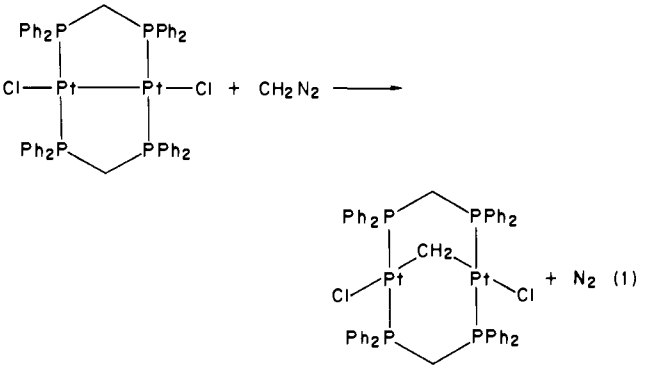

(1) Puddephatt, R. J. *Chem. Soc. Rev.* **1983**, *12*, 99.
(2) Balch, A. L. *Adv. Chem. Ser.* **1982**, *196*, 243.
(3) (a) Brown, M. P.; Fisher, J. R.; Franklin, S. J.; Puddephatt, R. J.; Thomson, M. A. *Adv. Chem. Ser.* **1982**, *196*, 231; (b) Balch, A. L. *ACS Symp. Ser.* **1981**, *155*, 167.
(4) Sanger, A. R. *Can. J. Chem.* **1982**, *60*, 1363.
(5) Kubiak, C. P.; Woodstock, C.; Eisenberg, R. *Inorg. Chem.* **1982**, *21*, 2119.
(6) (a) Brady, R. C., III; Pettit, R. *J. Am. Chem. Soc.* **1980**, *102*, 6181. (b) Brady, R. C., III; Pettit, R. *J. Am. Chem. Soc.* **1980**, *103*, 1287.
(7) Brown, M. P.; Puddephatt, R. J.; Rashidi, M.; Manojlovic-Muir, L.; Muir, K. W.; Solomun, T.; Seddon, K. R. *Inorg. Chim. Acta* **1977**, *23*, L33.
(8) Olmstead, M. M.; Hope, H.; Benner, L. S.; Balch, A. L. *J. Am. Chem. Soc.* **1977**, *99*, 5502.
(9) Brown, M. P.; Puddephatt, R. J.; Rashidi, M.; Seddon, K. R. *J. Chem. Soc., Dalton Trans.* **1978**, 1540.
(10) Brown, M. P.; Fisher, J. R.; Franklin, S. J.; Puddephatt, R. J.; Seddon, K. R. *J. Chem. Soc., Chem. Commun.* **1978**, 749.
(11) Benner, L. S.; Balch, A. L. *J. Am. Chem. Soc.* **1978**, *100*, 6099.
(12) Benner, L. S.; Olmstead, M. M.; Hope, H.; Balch, A. L. *J. Organomet. Chem.* **1978**, *153*, C31.
(13) Rattray, A. D.; Sutton, D. *Inorg. Chim. Acta* **1978**, *27*, L85.
(14) Brown, M. P.; Fisher, J. R.; Puddephatt, R. J.; Seddon, K. R. *Inorg. Chem.* **1979**, *18*, 2808.
(15) Muralidharan, S.; Espenson, J. H. *Inorg. Chem.* **1983**, *22*, 2786.

0002-7863/84/1506-8104$01.50/0

Reaction of $[Pt_2(PPh_3)_2(\mu\text{-dppm})_2]^{2+}$ [16] with any of several inserting reagents R (R = CH_2N_2, CO, SO_2, and S_8) leads to analogous but previously unknown complexes, the cationic A-frame species $[Pt_2(PPh_3)_2(\mu\text{-Y})(\mu\text{-dppm})_2]^{2+}$, with Y = CH_2, CO, SO_2, and S. A kinetic study of the latter reactions reveals substantial differences, however, and affords an opportunity to define the mechanism(s) in much finer detail. One possible interpretation of the kinetic data is that attack of R is preceded by unimolecular *heterolytic cleavage* of a bond within the binuclear complex. The feasibility of such a step, unprecedented as far as we are aware, was probed by several types of experiments. This paper reports kinetic and other measurements over a wide range of concentration variables, temperatures, solvents, and electrolytes.

Experimental Procedures

Materials. The complex $[Pt_2(PPh_3)_2(\mu\text{-dppm})_2](PF_6)_2$ was prepared as described[16] and characterized by ^1H and $^{31}P\{^1H\}$ NMR spectra which agreed with the reported spectra.[16] (^{31}P NMR spectra were recorded on a Bruker WM 300 spectrometer and ^1H NMR on a Nicolet, NT-300 spectrometer in the FT mode.) Methylene chloride was treated with sulfuric acid, sodium carbonate, and water and then distilled from phosphorus pentoxide. The solvent was stored over Fisher 4A molecular sieves, although independent measurements showed that small concentrations of water ($\sim 10^{-3}$–10^{-2} M) added to the reactions were without effect on the rate. Many measurements were made in air-saturated solvents after it was shown that exclusion of oxygen did not alter significantly the kinetics or products of the reactions. Other solvents—chloroform, acetone, and methanol—were distilled and stored over molecular sieves. Deuterated solvents for NMR spectra were dried over molecular sieves. The salts $N(n\text{-Bu})_4ClO_4$ and NEt_4Cl were recrystallized from ethanol and methylene chloride–acetone–hexane (2:2:1), respectively, and dried under vacuum.

Diazomethane was prepared from a Diazald Kit (Aldrich Chemical Co.). Stock solutions of CH_2N_2 in diethyl ether were stored in a refrigerator at −10 °C and standardized daily against benzoic acid.[17]

Saturated solutions of carbon monoxide and sulfur dioxide in dichloromethane were prepared by bubbling the gas through the solvent. The concentration of CO in the stock solution at a given temperature and pressure was taken from published tables.[18] Kinetic runs were conducted by injecting the desired volume of CO solution into a septum-capped quartz spectrophotometer cell filled so as to leave a minimum free volume. The reproducibility of the kinetic data at a given carbon monoxide concentration is taken to indicate that the value calculated from the dilution factor is close to the true value. The concentration of sulfur dioxide in dichloromethane was determined by iodometric titration.[19] Elemental sulfur was recrystallized twice from carbon disulfide and vacuum dried. Stock solutions of S_8 in carbon disulfide were prepared gravimetrically. It was found with use of $^{31}P\{^1H\}$ NMR that $[Pt_2(PPh_3)_2(\mu\text{-dppm})_2](PF_6)_2$ did not react with CS_2 even in solutions containing up to 30% CS_2.

Kinetic Determinations. Measurements were conveniently made by UV–visible spectrophotometry, since the parent complex exhibits strong absorption maxima at λ 404 and 350 nm with molar absorptivities of 1.55×10^4 and 2.30×10^4 M^{-1} cm^{-1}, respectively. In comparison, the A-frame products show less intense maxima or shoulders near 380 nm. The clean conversion of reactants to product without the intervention of any intermediate at a detectable concentration level is illustrated in Figure 1 for the insertion of CO. The maintenance of isosbestic points at λ 328 and 510 nm should be noted. Moreover, it is particularly important to note that the spectrum taken immediately upon mixing of the reagents is essentially that of the unreacted parent complex. This signals that no prior association between the reactants has occurred (or, at least, that any such association is not manifest by a change in the absorption spectrum, from which we tentatively conclude that none has occurred).

Numerical data for kinetic analysis were collected by monitoring the absorbance at a fixed wavelength as a function of time. Most reactions were monitored at 400 nm, but enough other measurements were made to establish that the rate constants were independent of the monitoring wavelength. A Cary Model 219 recording spectrophotometer with a water-filled cell holder maintained at ±0.1 °C was used for these measurements. In the presence of a large stoichiometric excess of the inserting reagent R the data followed pseudo-first-order kinetics and yielded values of k_{obsd} by the standard methods. Replicate runs were reproducible typically within 5%.

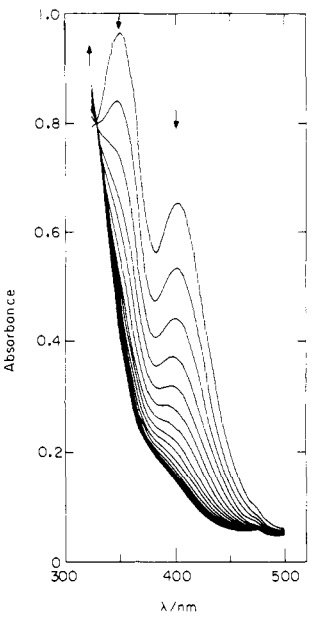

Figure 1. Scans of the UV–vis absorption spectrum during the reaction of $[Pt_2(PPh_3)_2(\mu\text{-dppm})_2](PF_6)_2$ (2×10^{-5} M) with CO (3.2×10^{-3} M) in CH_2Cl_2 at 5.0 °C. The spectra were recorded at intervals of 4.0 min in a cell of 2-cm optical path.

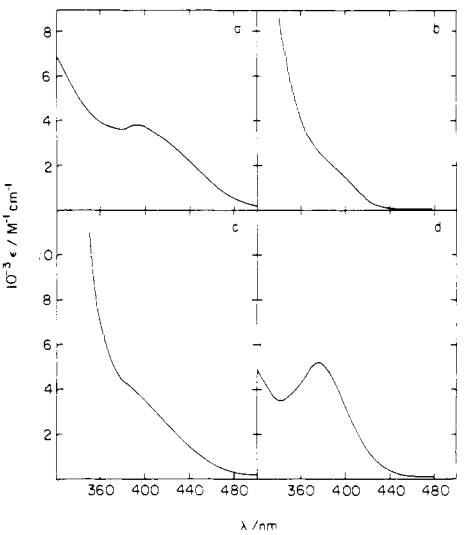

Figure 2. UV–vis spectra of the A-frame products $[Pt_2(PPh_3)_2(\mu\text{-Y})(\mu\text{-dppm})_2](PF_6)_2$ for Y = CH_2 (a), CO (b), and S_8 (c). The spectrum of $Pt_2Cl_2(\mu\text{-}CH_2)(\mu\text{-dppm})_2$ is also shown (d).

Results

The A-Frame Products. The reactions under investigation occur as in eq 2, to yield A-frame complexes. From reactions run at preparative-scale concentrations, the products are obtained as microcrystalline solids. At the concentrations used in kinetics

$$[Pt_2(PPh_3)_2(\mu\text{-dppm})_2](PF_6)_2 + R = [Pt_2(PPh_3)_2(\mu\text{-Y})(\mu\text{-dppm})_2](PF_6)_2 \quad (2)$$

R = CO, CH_2N_2, SO_2, and S_8; Y = CO, CH_2, SO_2, and S

experiments, they remain in solution in dichloromethane, in which they are quite soluble. The isolated materials and the complexes in solution are inferred to be the same since their UV–vis spectra are the same and also are characteristic (Figure 2) of other Pt_2 A-frame compounds in that they show absorption maxima or shoulders near 380 nm.

(16) Brown, M. P.; Franklin, S. J.; Puddephatt, R. J.; Thomson, M. A.; Seddon, K. R. *J. Organomet. Chem.* **1979**, *178*, 281.

(17) (a) *Aldrichimica Acta* **1970**, *3*, 9. (b) Procedure supplied by the Aldrich Chemical Co.

(18) Linke, W. R.; Seidell, A. "Solubilities of Inorganic and Metal Organic Compounds"; American Chemical Society: Washington, DC, 1958; Vol. I, pp 453–458.

(19) Charlot, G. "Quantitative Inorganic Analysis"; John Wiley and Sons: New York, 1957; pp 589–590.

Table I. ^1H and $^{31}P\{^1H\}$ NMR Parameters for A-Frame Compounds

complex	^1H NMR[a]		$^{31}P\{^1H\}$ NMR[b]			
	$\delta(CH_2)$/ppm[c]	^3J(Pt–H)/Hz	δ(dppm)/ppm	^1J(Pt–P)/Hz	$\delta(PPh_3)$/ppm	^1J(Pt–P)/Hz
$[Pt_2(PPh_3)_2(\mu\text{-dppm})_2](PF_6)_2$	5.6	60	−4.85	2857.8	17.76	1700
$[Pt_2(PPh_3)_2(\mu\text{-}CH_2)(\mu\text{-dppm})_2](PF_6)_2$	3.6	48	20.85	3587.0	32.76	1840.2
	5.0	12				
$[Pt_2(PPh_3)_2(\mu\text{-CO})(\mu\text{-dppm})_2](PF_6)_2$	3.8	53	−3.2	2591.2	21.6	1494.8
	5.2	11				
$[Pt_2(PPh_3)_2(\mu\text{-}SO_2)(\mu\text{-dppm})_2](PF_6)_2$	3.6	54	−5.1	3081	17.54	1680.3
	4.9	10				
$[Pt_2(PPh_3)_2(\mu\text{-S})(\mu\text{-dppm})_2](PF_6)_2$	4.0	58	7.46	3249	11.05	1544.2
	5.1	15				
$[Pt_2(PPh_3)_2(\mu\text{-H})(\mu\text{-dppm})_2](PF_6)_3$			−51.52[d]	3868	23.52	1798.4

[a] In $CDCl_3$ with Me_4Si reference. [b] In $CDCl_3$ with H_3PO_4 as external rerference. [c] For CH_2 of dppm; μ-CH_2 appears at δ 1.2 ppm [15]. [d] This value appears abnormal, but the ^1H NMR was inadequately resolved to permit a definitive answer.

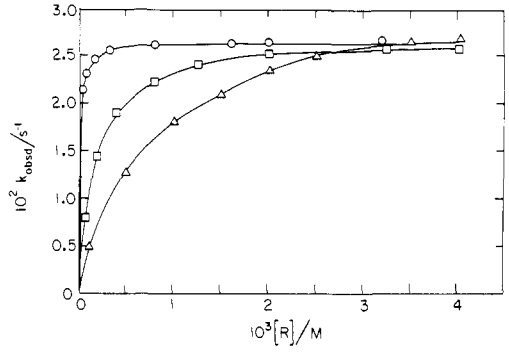

Figure 3. Plots showing the dependence of the pseudo-first-order rate constant for reactions of $[Pt_2(PPh_3)_2(\mu\text{-dppm})_2](PF_6)_2$ with various reagents R in dichloromethane at 25 °C. Values refer to CH_2N_2 (triangles), CO (circles), and S_8 (squares).

The isolated materials were shown to be A-frame compounds from the $^{31}P\{^1H\}$ and ^1H NMR spectra. The latter vary relatively little from one compound to the next; typically the CH_2 protons in the dppm ligands of $[Pt_2(PPh_3)_2(\mu\text{-Y})(\mu\text{-dppm})_2](PF_6)_2$, which are inequivalent in the A-frame structure,[14] occur as multiplets at δ ca. 3.6 and 5.05 ppm, relative to Me_4Si. The exact values and the ^{195}Pt coupling constants are given in Table I. The analysis parallels what has been done for analogous compounds[14] and need not be repeated in detail here. The $^{31}P\{^1H\}$ NMR spectra differ from one complex to the next, a feature also noted previously.[14] The chemical shifts and coupling constants, given in Table I, are also consistent with the A-frame structure.

The IR spectrum, examined during the reaction of carbon monoxide, showed the smooth growth of the frequency of the μ-CO group at ν = 1636 cm^{-1}. At no time during or after the main reaction was there any evidence for terminal CO absorption at 2072–2076 cm^{-1}, although examples of the latter are well-known[20,21] in such complexes as $[Pt_2(Cl)(CO)(\mu\text{-dppm})_2](PF_6)$ and $[Pt_2(CO)_2(\mu\text{-dppm})_2](PF_6)_2$.

Kinetics. The initial concentrations of the binuclear Pt(I) complex in kinetics experiments were quite low, 5×10^{-6}–2×10^{-4} M. The reagent R was present in large stoichiometric excess, the range of values depending upon the solubility and reactivity of the given compound. The reactions proceeded to completion and insofar as could be ascertained formed only the indicated A-frame product quantitatively. No evidence was obtained to suggest the presence of a reaction intermediate at a detectable concentration.

The pseudo-first-order rate constant was independent of the initial $[Pt_2(PPh_3)_2(\mu\text{-dppm})_2](PF_6)_2$ concentration over the range indicated.[19] The dependence of k_{obsd} was first order with respect to [R] in the limit of very low [R]. Over the entire concentration range, the dependence was more complex, since the rate tended toward a zero-order dependence on [R] at higher [R]. This is illustrated in Figure 3, which shows that in each case the rate reaches a plateau. In algebraic form the dependence of rate upon concentration is given by

$$\frac{d[\text{A-frame}]}{dt} = \frac{k[Pt_2(PPh_3)_2(\mu\text{-dppm})_2^{2+}][R]}{K + [R]} \quad (3)$$

This rate equation requires that a double-reciprocal plot (k_{obsd}^{-1} vs. $[R]^{-1}$) be linear. The plots are shown in Figure 4. Fitting

$$\frac{1}{k_{obsd}} = \frac{1}{k} + \frac{K}{k[R]} \quad (4)$$

of each data set to eq 3 with use of a nonlinear least-squares analysis yielded the values of k and K given in Table II. The limiting rate constant at high [R] corresponds to the parameter k of eq 2–4. Particularly key to the interpretation is the finding that the value of k is independent, within the experimental pre-

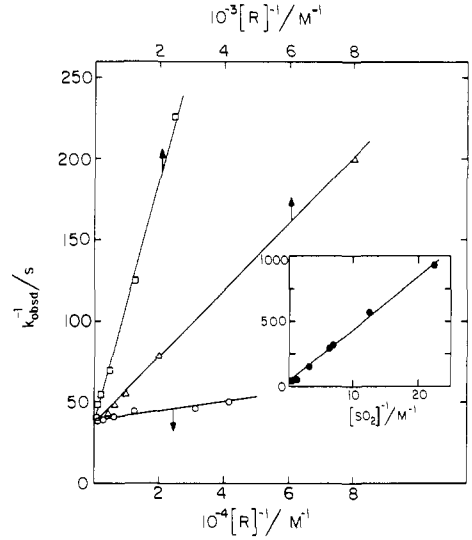

Figure 4. Double reciprocal plots of the kinetic data illustrating the linear dependence of $1/k_{obsd}$ vs. $1/[R]$. Data are as shown in Figure 3 except that data for the SO_2 reaction (filled circle) have been added.

Table II. Kinetic Parameters[a,b] for the Reactions of $[Pt_2(PPh_3)_2(\mu\text{-dppm})_2](PF_6)_2$ with Reagents R in Dichloromethane at 25.0 °C

R	range of [R]	$10^2k/s^{-1}$	K/mol dm^{-3}
CH_2N_2	$(0.13\text{–}20) \times 10^{-3}$	2.97 ± 0.05	$(6.2 \pm 0.3) \times 10^{-4}$
CO	$(0.24\text{–}32) \times 10^{-4}$	2.56 ± 0.03	$(6.5 \pm 0.6) \times 10^{-6}$
S_8	$(0.4\text{–}40) \times 10^{-4}$	2.74 ± 0.06	$(2.0 \pm 0.1) \times 10^{-4}$
SO_2	0.04–1.6	2.8 ± 0.3[c]	1.1 ± 0.2
		av 2.73 ± 0.05[c]	

[a] From a nonlinear least-squares fit of the data to eq 3; uncertainties represent one standard deviation. [b] The interpretation suggests $k = k_1$ and $K = k_{-1}/k_2$ in Scheme I. [c] The less precise system (SO_2) was excluded from the averaging.

(20) Puddephatt, R. J.; Azam, K. A.; Hill, R. H.; Brown, M. P.; Nelson, C. D.; Moulding, R. P.; Seddon, K. R.; Grossel, M. C. *J. Am. Chem. Soc.* **1983**, *105*, 5642.

(21) Fisher, J. R.; Millis, A. J.; Summer, S.; Brown, M. P.; Thomson, M. A.; Puddephatt, R. J.; Frew, A. A.; Manojlovic-Muir, L.; Muir, K. W. *Organometallics* **1982**, *1*, 1421.

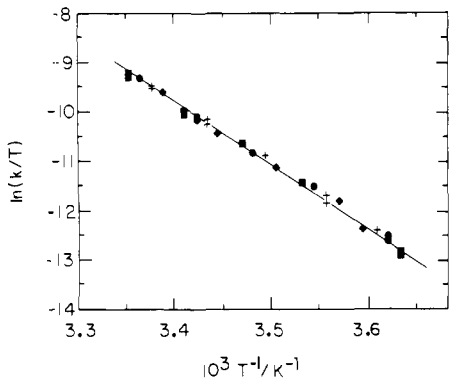

Figure 5. Analysis of the temperature dependence of the limiting first-order rate constant k according to activated complex theory. The different symbols refer to data for R = CH_2N_2 (squares), CO (circles), S_8 (pluses), and SO_2 (diamonds).

cision, of the nature of R. This is substantiated by the common plateau in Figure 3, the common intercept in Figure 4, and the least-squares values in Table II, which give an average value, k = (2.73 ± 0.05) × 10^{-2} s^{-1} at 25.0 °C in dichloromethane.

Other kinetics experiments in which CO and the Pt_2 complex were present at comparable concentrations will be considered in the Interpretation and Discussion.

Variation of Temperature. The constancy of k, irrespective of [R], is not an accidental occurrence at the one temperature employed. Similar determinations were conducted at other temperatures (2–32 °C) in dichloromethane. In each case the value of k was the same at a given temperature, as indicated by the plot of ln (k/T) vs. $1/T$, according to activated complex theory, shown in Figure 5. A least-squares analysis of these data yields the activation parameters $\Delta H^{\ddagger}$ = 25.0 ± 0.3 kcal mol^{-1} and $\Delta S^{\ddagger}$ = 18.4 ± 0.9 cal mol^{-1} K^{-1}.

Effects of "Inert Salts" and the Insertion of H^+ by Reaction with HCl. Treatment of $[Pt_2(PPh_3)_2(\mu\text{-dppm})_2](PF_6)_2$ with anhydrous HCl in CH_2Cl_2 yields an A-frame product, isolable upon addition of NH_4PF_6 as $[Pt_2(PPh_3)_2(\mu\text{-H})(\mu\text{-dppm})_2](PF_6)_3$. The kinetics of this reaction in dichloromethane also were in accord with eq 3 and 4, the kinetic parameters at 25 °C being k = (4.17 ± 0.02) × 10^{-2} s^{-1} and K = (1.77 ± 0.03) × 10^{-3} M. This value of k is some 50% higher than the others, although the algebraic dependence for R = HCl has the same form.

To test whether the variation of k signaled a change in mechanism, a kinetic study of the reaction with R = CO was undertaken with added salts. The value at 25 °C in dichloromethane of k, the limiting first-order rate constant at high [CO], increased steadily from 2.7 × 10^{-2} s^{-1} up to 6.0 × 10^{-2} s^{-1} [≥1 × 10^{-3} M $N(n\text{-Bu})_4ClO_4$].[22] Beyond this limit the rate constants were insensitive to further addition of $R_4N^+X^-$. In dichloromethane the reactant complex almost certainly exists as the ion pair $[Pt_2(PPh_3)_2\text{-}(\mu\text{-dppm})]_2(X)_2$. The change from X = PF_6^- to ClO_4^- probably gives rise, by virtue of the different species predominant in solution, to the changes in reactivity noted.

Solvent Variations. The reaction between $[Pt_2(PPh_3)_2(\mu\text{-dppm})_2](PF_6)_2$ and CO was investigated in several solvents. These measurements were carried out at high [CO], so as to obtain the value of the limiting rate constant k of eq 3. (The [CO] independence was verified.) The value of k decreases as solvents of higher polarity are used, Table III. They vary with dielectric constant (D) as depicted in Figure 6, which shows that ln k is a linear function of $1/D$. In this range of solvents the reactant complex changes over from an ion pair to a free dispositive ion. In each instance, however, it was confirmed by ^{31}P NMR and by IR that the same A-frame product with a μ-CO group is formed.

(22) Measurements made in the presence of NEt_4Cl, which gave k_{lim} = 4.15 × 10^{-2} s^{-1}, are not strictly comparable, since conversion to $[Pt_2Cl(PPh_3)(\mu\text{-dppm})_2]^+$ was complete prior to A-frame formation (R. J. Blau and J. H. Espenson, unpublished results). The reaction with HCl, however, leads directly to an A-frame complex with terminal PPh_3 (not Cl^-) ligands, $[Pt_2(PPh_3)_2(\mu\text{-H})(\mu\text{-dppm})_2^{3+}]Cl_3$, as shown by NMR.

Table III. Values of the Limiting Rate Constant[a,b] k in Solvents of Different Polarity

solvent	dielectric constant	$10^2k^b/s^{-1}$
$CHCl_3$	4.81	13.3
CH_2Cl_2	9.08	2.73
$(CH_3)_2CO$	20.7	2.13
CH_3OH	32.6	0.74
$H_2O\text{-}(CH_3)_2CO$[c]	50.3	0.61

[a] At 25.0 °C. [b] The parameter k is identified as k_1 as Scheme I (see Discussion). [c] A 1:1 mixture by volume.

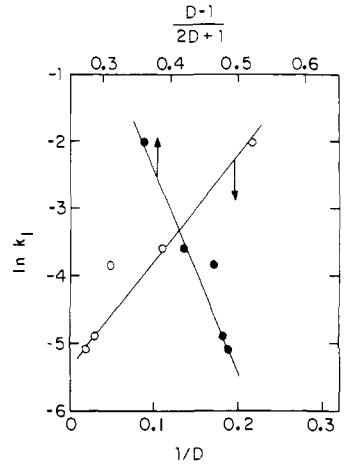

Figure 6. The effect of solvent polarity on the value of the limiting rate constant, k_1, illustrated by a plot of ln k_1 vs. $1/D$ (open circles) and vs. $(D - 1)/(2D + 1)$.

Addition of modest concentrations of water to the reactions of CO in dichloromethane had no effect on the rate constant. The reactant and product are unaffected by water, and the limiting first-order rate constant at high [CO] remains invariant, 2.64 × 10^{-2} s^{-1} (0.03 M H_2O) and 2.81 × 10^{-2} s^{-1} (0.10 M), as compared to 2.56 × 10^{-2} s^{-1} (without added water).

Effects of Oxygen, Alkyl Halide, and Triphenylphosphine Additions. The rate of reaction of CO (1.6 × 10^{-3}–3.2 × 10^{-3} M) with 5 × 10^{-6}–10^{-4} M $[Pt_2(PPh_3)_2(\mu\text{-dppm})_2](PF_6)_2$ at 25 °C was little affected by the presence of 0.1 M $PhCH_2Br$, $PhCH_2Cl$, and $CHBr_3$. The product was still $[Pt_2(PPh_3)_2(\mu\text{-CO})(\mu\text{-dppm})_2](PF_6)_2$ immediately after this reaction as shown by IR (1636 cm^{-1}) and $^{31}P\{^1H\}$ NMR. When, however, $[Pt_2(PPh_3)_2(\mu\text{-dppm})_2](PF_6)_2$ was allowed to react with the above halides at concentrations of halides ≥1 M, a slow reaction occurred. For example, $PhCH_2Br$ reacted with 10^{-5} M complex with k_{obsd} = 1.2 × 10^{-2} s^{-1} and several products could be identified in the ^{31}P NMR. The formation of these products may or may not involve the intermediate responsible for "A"-frame formation. Further detailed studies with the above halides are necessary to understand these reactions.

Kinetic experiments were also carried out with added PPh_3 in the reactions of $[Pt_2(PPh_3)_2(\mu\text{-dppm})_2](PF_6)_2$ with CH_2N_2 (0.004–0.01 M) and CO (1.6 × 10^{-3} M). The former yields k (25 °C in CH_2Cl_2) = 2.75 × 10^{-2} s^{-1} (0.010 M PPh_3) and 2.72 × 10^{-2} s^{-1} (0.10 M PPh_3); the latter yields 2.65 × 10^{-2} s^{-1} (0.10 M PPh_3). All of the values are within experimental error of those (Table II) for the same reaction without added phosphine. Oxygen has no effect on the reactions. Experiments in which air was replaced by an atmosphere of Ar or of pure O_2 proceeded at the same rate.

Product Ratio. In defining the mechanism, it was considered instructive to examine the A-frame products formed when the starting complex was allowed to react in the presence of two reagents R. The question is whether the two A-frame products are formed in a ratio which agrees with their relative rates of formation as determined separately.

In such an experiment, the complex (1.0 mM) was reacted with a mixture of CO (initial concentration 5.0 mM; average concentration 4.58 mM) and S_8 (initial and average concentration

Scheme I

$$Pt_2(PPh_3)_2(\mu\text{-dppm})_2^{2+} \underset{k_{-1}}{\overset{k_1}{\rightleftharpoons}} Int_1 \quad \text{(I-1)}$$

$$Int_1 + R \xrightarrow{k_2} Pt_2(PPh_3)_2(\mu\text{-Y})(\mu\text{-dppm})_2^{2+} \quad \text{(I-2)}$$

$$k_{obsd} = \frac{k_1[R]}{(k_{-1}/k_2) + [R]} \quad \text{(I-3)}$$

Scheme II

$$Pt_2(PPh_3)_2(\mu\text{-dppm})_2^{2+} + R \underset{}{\overset{K}{\rightleftharpoons}} \text{adduct} \quad \text{(II-1)}$$

$$\text{adduct} \xrightarrow{k'} Pt_2(PPh_3)(\mu\text{-Y})(\mu\text{-dppm})_2^{2+} \quad \text{(II-2)}$$

$$k_{obsd} = \frac{k'[R]}{K^{-1} + [R]} \quad \text{(II-3)}$$

Scheme III

$$Pt_2(PPh_3)_2(\mu\text{-dppm})_2^{2+} + R \underset{}{\overset{K}{\rightleftharpoons}} \text{adduct} \quad \text{(III-1)}$$

$$Pt_2(PPh_3)_2(\mu\text{-dppm})_2^{2+} + R \xrightarrow{k''} Pt_2(PPh_3)_2(\mu\text{-Y})(\mu\text{-dppm})_2^{2+} \quad \text{(III-2)}$$

$$k_{obsd} = \frac{k''K^{-1}[R]}{K^{-1} + [R]} \quad \text{(III-3)}$$

33.0 mM). The products are formed in a ratio of $[\mu\text{-CO}]_\infty/[\mu\text{-S}]_\infty = 5.5 \pm 0.2$, as determined by the areas of their peaks in the ^{31}P spectrum. The theoretical value, assuming that they are formed independently, is given by eq 5. In its derivation it has been

$$[\mu\text{-CO}]_\infty/[\mu\text{-S}]_\infty = K_S[CO]_{av}/K_{CO}[S_8]_{av} \quad (5)$$

assumed that the values of the numerator rate constant k of eq 3 are identical for the two (See Table II) and that [CO] and [S_8] are sufficiently constant that use of an average value suffices. On such a basis the calculated ratio is 4.3 ± 0.6. Within the experimental error, this agrees with the ratio determined.

Interpretation and Discussion

Plausible Mechanisms. All the reactions follow the rate equation

$$\frac{-d\ln[Pt_2(PPh_3)_2(\mu\text{-dppm})_2(PF_6)_2]}{dt} = k_{obsd} = \frac{k[R]}{K + [R]} \quad (6)$$

The fact that the observed rate constant reaches a limiting value at a sufficiently high [R] is indicative of a mechanism consisting of a multistep reaction sequence. One such sequence has as its first step a unimolecular reaction of the original Pt_2 complex. That step yields an intermediate which either returns to the starting material or reacts with the inserting reagent R. Deferring for the moment what the character of that intermediate may be, we show a mechanism of this general form in Scheme I.

Equally consistent with the kinetic data at high [R] are mechanisms in which the parent complex and R enter into a prior rapid equilibrium. It is the saturation of that equilibrium at sufficiently high [R] which causes the rate to attain a limiting plateau. Two such formulations are possible. In the one, Scheme II, the adduct formed as a result of the interaction lies along the reaction path, and its unimolecular rearrangement leads to the A-frame product. In the other, Scheme III, the adduct forms to the same extent, but it is a nonproductive species. That is, A-frame formation occurs by direct reaction of R, without involvement of the adduct. The latter acts as a nonproductive storage depot, thereby lowering the rate.

As can be seen from the kinetic equations shown with each mechanism, the experimental rate law obtained in the presence of a large excess of R is the same for all three. Clearly, then, a decision between them cannot be made on that basis.

One telling point, clearly in support of Scheme I, lies in the value of the limiting rate constant k. As noted earlier, its value at each temperature is the same for each reaction system (Table II and Figure 5). In Scheme I, this parameter is identified as k_1, the rate of unimolecular rearrangement. The constancy of k follows naturally since, in Scheme I, R is not involved at that point.

On the other hand, in either of the mechanisms involving adduct pre-formation, the reasons that k might be independent of the nature of R are quite obscure. In Scheme II, for example, k is identified as k', referring to A-frame formation from the R-containing adduct. It is strained, indeed, to suggest that such constancy might be a characteristic of these systems, particularly when one considers the very wide range of the chemical identities of the R's considered.

Other arguments can also be advanced and more chemical reasons invoked as well, but before considering these in any further detail we turn to the analysis of experiments in which Schemes I, II, and III do not all lead to the same rate law.

Kinetic Experiments and Simulations at Low [R]. The derivations which accompany the mechanisms shown in Schemes I–III are valid with $[R] = [R]_0$ only for experiments run under pseudo-first-order conditions, $[R]_0 \gg [Pt_2(PPh_3)_2(\mu\text{-dppm})_2^{2+}]_0$. For these two types of mechanisms, however, [R] changes in a different fashion throughout the run. Thus in Scheme I, $[R]_t = [R]_0 - \Delta_t$, where Δ_t represents the concentration of A-frame product formed at each point in time ($\Delta t = [Pt_2(PPh_3)_2(\mu\text{-dppm})_2^{2+}]_0 - [Pt_2(PPh_3)_2(\mu\text{-dppm})_2^{2+}]_t$). On the other hand, in Schemes II and III, the concentration of free R at $t = 0$ is lower than the initial or total value, owing to the sudden burst of adduct formed in the rapid equilibration step.

This means that kinetic experiments under conditions where R is not added in a large initial excess over the dinuclear platinum complex will yield a distinctly different profile for product formation with time. Since the integrated forms of these rate laws not only are complex but also yield functional forms not amenable to ready comparison, we adopted a different approach to analyze the results by each of the two models.

We employed a program called KINSIM,[23] which provides concentration–time data for any given mechanism when the numerical values of the rate and equilibrium constants are supplied. (It employs suitable numerical integrations, such as the Runge–Kutta and Gear methods, depending on the features of a given scheme and the "stiffness" of the differential equations.) The results of the simulation were then compared with the data, to discern which, if any, of the schemes matched.

The most meaningful comparison is made in terms of absorbances, the quantity measured experimentally. In Scheme I, this presents no difficulty; the intermediate is present at steady-state concentration, and thus does not contribute, whereas the reactant and product have precisely known molar absorptivities. In Schemes II and III, however, where the "adduct" will attain concentrations comparable to those of reactant and product, the choice of its molar absorptivity becomes a matter of some importance. Hence we chose for A a set of values ranging from 20 to 6×10^4 M^{-1} cm^{-1} at 400 nm.

The results of such a simulation for one kinetic run are depicted in Figure 7. In that experiment the initial concentrations of $Pt_2(PPh_3)_2(\mu\text{-dppm})_2^{2+}$ and of CO (the R used) were comparable, 16.4 and 8.0 μM, respectively. The experimental absorbance–time curve matches that simulated according to Scheme I, using the known kinetic parameters (Table II) derived from experiments in which CO was present in large excess. In contrast, no match could be attained between the experimental curve and that simulated for either Scheme II or III, regardless of the molar absorptivity value assumed for the adduct. Analogous findings were obtained for several other concentrations and choices of R, leading us to reject *for this system* (in which the bulky PPh_3 ligands are present) any mechanism involving pre-equilibrium adduct formation, either lying along the path to product, as in Scheme II, or coincidental to it, as in Scheme III.

The Chemical Mechanism. The mechanism shown in Scheme I is the only one of those considered which fits kinetic and other

(23) Barshop, B. A.; Wrenn, R. F.; Frieden, C. *Anal. Biochem.* **1983**, *130*, 134.

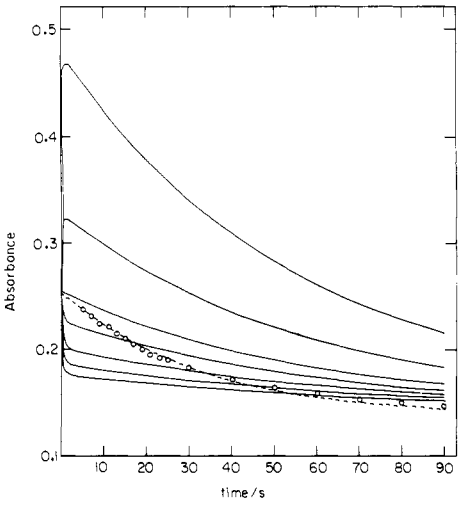

Figure 7. Simulated absorbance–time profiles for two classes of mechanism compared with experimental data (circles) for an experiment having comparable initial concentrations of $[Pt_2(PPh_3)_2(\mu\text{-dppm})_2](PF_6)_2$ (16.4 μM) and CO (8.0 μM). The dashed line represents the simulated tracing for Scheme I and solid curves for Schemes II and III. In both cases the kinetic parameters (k and K) are those taken from experiments in which CO is present in large excess, as in Table II. Various values were assumed for the molar absorptivity of the equilibrated adduct from 20 (lowest curve) to 6×10^4 (highest), but none of these provides a satisfactory fit to the experimental data.

data under all conditions. The mechanism in the generalized form shown does not specify the chemical nature of the intermediate which is obtained from, and returns to, the starting complex in unimolecular reactions. There are several possibilities for the nature of the intermediate Int_1; ignoring species derived via conformational or isomeric transformations, it seems four alternatives can be envisaged, as follows:

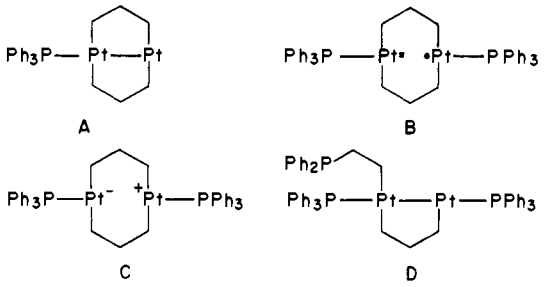

Dissociation of terminal PPh_3 (A) can be discounted because the reverse transformation (k_{-1} step) would not follow first-order kinetics and because k_{obsd} proved unaffected by the addition of PPh_3. The homolytic dissociation of the metal–metal bond to form a pair of Pt-centered radicals (B) seems most unlikely. The reaction products and rate are unaffected by added O_2 or organic halide; in addition, the reagents R which are effective in A-frame formation do not appear to be particularly well constituted to react with a metal-centered radical.

A unimolecular bond heterolysis appears to offer a more attractive alternative. Not so easily decided, however, is whether the bond so cleaved is the metal–metal bond resulting in simultaneous 16-e and 14-e centers (C) or the bond between a platinum and one arm of the briding dppm ligand (D).

The former might be argued *against* because the reaction is insensitive to moisture, whereas species C might be expected to react readily with H_2O. The alternative D is appealing *in this special case where severe steric crowding about each platinum atom results from the seven phenyl groups supplied by the three phosphine donors*. Formation of D clearly relieves this difficulty, providing room for attack of R. (It should be noted, however, that the product isolated in every instance contains only intact $Pt_2(\mu\text{-dppm})_2$ units, necessarily implying that this bond, if broken as suggested in D, is reconstituted efficiently in a later reaction.)

One other appealing aspect of formulation D is that it would be expected to offer a preferred pathway only for the case in which steric considerations block a more efficient transformation. That feature is also important because analogous insertions of R into the Pt–Pt bond of $Pt_2Cl_2(\mu\text{-dppm})_2$ and similar compounds do *not* show analogous kinetic profiles,[15,24] implying that bond opening prior to reaction of R is not a prerequisite in those instances. The solvent effects observed might arise from ground-state (i.e., ion pairing vs. ionization) or transition-state effects, and thus they do not appear to offer a resolution in this instance.

The activation parameters associated with k_1 are $\Delta H^{\ddagger} = 25.0 \pm 0.3$ kcal mol^{-1} and $\Delta S_1^{\ddagger} = +18.4 \pm 0.9$ cal mol^{-1} K^{-1}. These values are quite plausible for ligand dissociation, with the large, positive value of $\Delta S^{\ddagger}$ providing additional support for a scheme in which platinum–phosphine dissociation occurs. Again, however, they lie also in the range expected for other bond dissociation processes and are perhaps not compelling evidence for any of structures A–D.

Conformational changes within the extended cyclohexane-like unit of the starting complex have been observed in related complexes.[20] These occur on the NMR time scale, however. It is thus unlikely that the k_1/k_{-1} transformation yields an intermediate which differs from the reactant only in conformation. First, the rate constant k_1 appears too high ($k_1 = 0.027$ s^{-1} at 25 °C or $\Delta G_{298}^{\ddagger} = 19.7$ kcal mol^{-1}). In addition, the large value of $\Delta H^{\ddagger}$ suggest bond breaking, not conformational change, in the initial step.

According to Scheme I, the experimental parameter K is identified as the rate constant ratio k_{-1}/k_2. Since k_{-1} is common to all the reactants, the values of $1/K$ permit an assessment of the reactivity of each molecule R with the bond-opened intermediate. Relative to the slowest of these values, arbitrarily set to unity, the reactivities are the following: SO_2 (1), HCl (6×10^2), CH_2N_2 (1.8×10^3), S_8 (5.5×10^3), and CO (1.7×10^5). To interpret these data, it needs to be recognized that the character of the k_2 step may well change along the series, depending on the chemical character of R. That is, this step may in some cases (e.g., S_8, CO) represent attack *by* R on the newly created electron-deficient metal center of D; in others, however, it may represent attack *on* R by the electrons in the metal–metal bond. The latter is particularly attractive for the reagents normally function primarily as Lewis acids (e.g., HCl, SO_2). One fascinating detail in this context is the question of how an S atom is extracted so efficiently from the S_8 molecule. This point is better considered in our studies[24] of the related $Pt_2Cl_2(\mu\text{-dppm})_2$ system, where the initial k_1, k_{-1} step is not present to complicate the picture.

Acknowledgment. This work was supported by the U.S. Department of Energy, Office of Basic Energy Sciences, Chemical Sciences Division, under contract W-7405-ENG-82. We are grateful to Professor C. Frieden for supplying a copy of the KINSIM program and to Mr. Dee Huang for assistance with the NMR measurement. The Nicolet-NT-300 spectrometer was purchased with partial support from NSF Grant No. CHE-3209709.

Registry No. $[Pt_2(PPh_3)_2(\mu\text{-dppm})_2](PF_6)_2$, 69215-88-9; $[Pt_2(PPh_3)_2(\mu\text{-}CH_2)(\mu\text{-dppm})_2](PF_6)_2$, 86993-73-9; $[Pt_2(PPh_3)_2(\mu\text{-CO})(\mu\text{-dppm})_2](PF_6)_2$, 93473-51-9; $[Pt_2(PPh_3)_2(\mu\text{-}SO_2)(\mu\text{-dppm})_2](PF_6)_2$, 93473-53-1; $[Pt_2(PPh_3)_2(\mu\text{-S})(\mu\text{-dppm})_2](PF_6)_2$, 93454-07-0; $[Pt_2(PPh_3)_2(\mu\text{-H})(\mu\text{-dppm})_2](PF_6)_2$, 93454-09-2; CH_2N_2, 334-88-3; CO, 630-08-0; S, 7704-34-9; SO_2, 7446-09-5; HCl, 7647-01-0.

(24) Muralidharan, S.; Espenson, J. H., to be published.